Dinitrogen activation by zirconium dimer loaded C60

Kuganathan, N., Fossati, P. C. M., Gkanas, E. & Chroneos, A.

Original citation:
Kuganathan, N, Fossati, PCM, Gkanas, E & Chroneos, A 2019, 'Dinitrogen activation by zirconium dimer loaded C60', AIP Advances, vol. 9, 055331.
https://dx.doi.org/10.1063/1.5106430

DOI 10.1063/1.5106430
ESSN 2158-3226

Publisher: AIP Publishing

AIP Advances

Dinitrogen activation by zirconium dimer loaded C_{60}

Cite as: AIP Advances **9**, 055331 (2019); https://doi.org/10.1063/1.5106430
Submitted: 28 April 2019 . Accepted: 21 May 2019 . Published Online: 31 May 2019

Navaratnarajah Kuganathan, Paul C. M. Fossati, Evangelos Gkanas, and Alexander Chroneos

Dinitrogen activation by zirconium dimer loaded C_{60}

Cite as: AIP Advances 9, 055331 (2019); doi: 10.1063/1.5106430
Submitted: 28 April 2019 • Accepted: 21 May 2019 •
Published Online: 31 May 2019

Navaratnarajah Kuganathan,[1,2,a)] Paul C. M. Fossati,[1] Evangelos Gkanas,[2] and Alexander Chroneos[1,2]

AFFILIATIONS

[1] Department of Materials, Imperial College London, London SW7 2AZ, United Kingdom
[2] Faculty of Engineering, Environment and Computing, Coventry University, Priory Street, Coventry CV1 5FB, United Kingdom

[a)] Corresponding author, e-mail: n.kuganathan@imperial.ac.uk

ABSTRACT

Dinitrogen activation plays an important role in the production of many essential nitrogen based compounds needed for all life. Using density functional theory together with dispersion correction (DFT+D), the activation of molecular nitrogen with a gas phase Zr dimer and a Zr dimer loaded C_{60} is investigated. The present calculations show that the optimised *trans*-Zr_2N_2 configuration is planar but this configuration exhibits a butterfly shape when it is supported by C_{60}. Furthermore, it is shown that the activation of dinitrogen is facilitated by the Zr dimer stabilized by C_{60}. Additional calculations are carried out to look at the products of the reactions with H_2 and a catalytic cycle for the reduction of N_2 to NH_3 is constructed. Reaction of two molecules of H_2 with Zr_2N_2 molecule loaded C_{60} is exothermic while reaction of only one molecule of H_2 with *free* Zr_2N_2 molecule is exothermic again highlighting the importance of stabilization with C_{60}.

I. INTRODUCTION

Molecular nitrogen (N_2) is the most abundant component of the atmosphere on Earth and is an essential element in the chemistry of life. Due to its high bond strength (N≡N triple bond length = 109.768 pm and dissociation energy D_0 = 941.7 kJ mol^{-1}),[1] it is very difficult to oxidize or reduce. Though the inertness of dinitrogen is useful in chemical reactions in the absence of air and water, a wide variety of reactions are also considered to dissociate strong N_2 triple bond for the formation of useful products.

Dinitrogen activation is an important process in the cleavage of the N_2 triple bond. This process is fundamentally important for the synthesis of nitrogen-containing molecules essential for all life. The Haber process[2] is the principal industrial process for N_2 activation. In this successful commercial process, N_2 reacts with three equivalents of H_2 gas over a metal catalyst to yield ammonia. It is a large scale process with high energy demands and associated transport costs. Dinitrogen has also been activated by a class of enzymes called nitrogenases in biological systems,[3–5] soluble metal complexes[6–9] and bare transitional dimers in matrix isolation experiments.[10–12]

Matrix (chemically inert substance) isolation technique, a powerful experimental tool to study the reactive species and their intermediates, has been used to activate dinitrogen by reacting bare transition metal atoms and dimers giving important insight into the bonding properties and mechanisms.[10–12] For example, matrix isolation experiments were used to synthesize and characterize the Ti dimer at low temperature using noble gas as matrix.[10] Complete cleavage of the strong N≡N strong triple bond by the reaction of Ti_2 with N_2 in a single step in noble gas matrix was reported by Hans-Jörg Himmel *et al.*[13,14] The successful cleavage of N_2 molecule with Ti_2 dimer in noble gas matrices led to enormous interest in developing new catalytically active materials that can stabilize metal atoms or dimers for dinitrogen activation.

The buckyball structured carbon fullerenes (C_{60}) are promising candidate materials for developing catalytically active materials as they have outer surface structures with very high mechanical stability at higher pressures and temperatures.[15,16] Considerable research effort has been carried out on the catalytic activity of metal or metal clusters absorbed C_{60} system.[17–21] For example, titanium decorated C_{60} was considered as an efficient storage media for hydrogen because of the weak bonding nature between pure C_{60} and hydrogen.[22] In a previous study,[23] we proposed the possibility of

Ti_2 loaded C_{60} as a promising stable system for splitting dinitrogen molecule.

Experimental reaction between lazer–ablated Zr and N_2 has been reported and the resultant structure exhibits a four-membered cyclic $Zr_2(\mu\text{-}N_2)$ species with D_{2h} symmetry as observed for Ti_2N_2.[24] However, there is no report on the stabilisation of Zr dimer with C_{60} and its reactivity with N_2. In the present study, plane wave based density functional theory with dispersion correction (DFT+D) is applied to examine the reactivities of gas phase Zr dimer and Zr dimer chemisorbed on C_{60} with molecular nitrogen. Additional calculations were carried out to examine the products of the reactions with H_2 leading to the formation of NH_3. Structural details, reaction energies, a catalytic cycle for reduction of N_2 to NH_3 with Zr_2C_{60} as catalyst and relative energies of the intermediates formed during the reaction $N_2 + 3H_2 \rightarrow 2NH_3$ are reported. Furthermore, the hydrogenated products of the *free* Zr_2N_2 molecule and their reaction energies are compared to that of $Zr_2N_2C_{60}$.

II. COMPUTATIONAL METHODS

The calculations are based on density functional theory. The VASP code,[25,26] which performs this calculation solving the standard Kohn-Sham (KS) equations, was used. The exchange and correlation term was modelled using the generalized gradient approximation (GGA) parameterized by Perdew, Burke, and Ernzerhof (PBE).[27] In all cases we have used a plane-wave basis set with a cut off value of 500 eV. Structural optimizations were performed in all calculations using conjugate a gradient algorithm[28] until the residual forces were always smaller than 0.001 eV/Å. A single k-point (Γ) point was used in all calculations to represent the Brillouin zone due to the large super cell. Cubic supercells with 25 Å were used in all calculations to ensure that the two adjacent structures do not interact with each other. The same supercell was used to calculate the energies of N_2, H_2 and NH_3 molecules. Reaction energies were calculated using the following equation (1)

$$E_r = E(M\text{-}C_{60}) - E(C_{60}) - E(M) \quad (1)$$

where E (C_{60}) is the total energy of a pristine C_{60} molecule, E (M-C_{60}) is the total energy of a molecule interacting C_{60} and E (M) is the total energy of an isolated molecule.

Here, van der Waals (vdW) interactions were included by using the pair-wise force field as implemented by Grimme *et al.*[29] in the VASP package. The efficacy of the pseudopotentials and basis sets for C were tested and reported in our recent theoretical work.[30] The calculated bond distances of gas phase N_2 and H_2 were 1.12 Å and 0.75 Å respectively. These values agree well with the corresponding experimental values of 1.10 Å[31] and 0.74 Å[32] indicating that the efficacy of the pseudopotentials and basis sets used for N and H.

III. RESULTS AND DISCUSSIONS

A. The formation of *cis*- and *trans*-Zr_2N_2 complexes from gas phase Zr_2 and N_2

Molecular structures of Zr_2N_2 in the form of *cis* and *trans* configurations were first optimised. Figure 1 shows the resultant

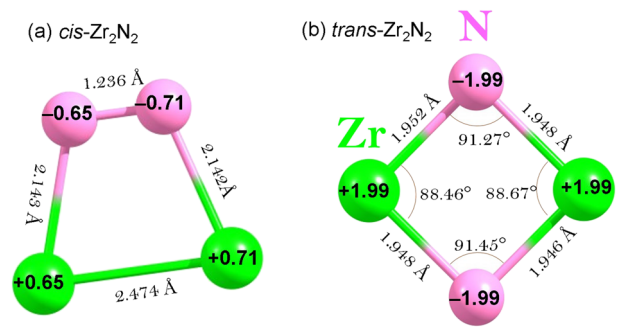

FIG. 1. DFT optimised structures of *cis*- and *trans*-Zr_2N_2 together with structural parameters and Bader charges on Zr and N atoms.

DFT optimised structures together with the bond distances and Bader charges. In the *cis* configuration, N_2 laterally interacts with Zr dimer forming a cyclic structure. A bond elongation of 0.13 Å in the N_2 molecule is observed compared to the value calculated for gas phase N_2. The Zr-Zr bond distance also increases by 0.46 Å compared to its gas phase Zr dimer. This clearly indicates that N_2 molecule is activated by Zr dimer but the degree of activation did not lead to the cleavage of N_2 molecule. The Bader charge analysis shows there is a charge transfer (1.36 |e|) from the Zr dimer to the N_2 molecule forming strong bonds between Zr and N. The reaction energy for the formation of *cis*-Zr_2N_2 from N_2 and Zr_2 is −143.8 kJmol^{-1} suggesting that this process is thermodynamically favourable.

The optimised structure of *trans*-Zr_2N_2 [Zr(μ-N)$_2$Zr] is planar and cyclic with alternating Zr and N atoms as observed for the Ti_2N_2 in the experiment[10] and previous theoretical DFT calculations.[23] In the optimised structure the Zr-N bond length is ~1.95 Å which is 0.15 Å and 0.20 Å longer than the calculated and experimental Ti-N bond length values, respectively. The N-Zr-N and Zr-N-Zr bond angle values are ~88.5° and ~91.0° respectively. These values are closer to the corresponding values calculated for *trans*-Ti_2N_2 (87.3° and 92.7°). The longer distances indicate that Zr-N bond strength is weaker than that of Ti-N. This is because of the larger atomic radius of Zr than that of Ti.

The Zr-Zr and N-N separations are 2.79 Å and 2.72 Å respectively in our present calculations. The N-N separation clearly indicates that there is no direct interaction between the two N atoms. The formation of a Zr_2N_2 molecule from Zr_2 and N_2 is associated with an energy change of −440 kJ mol^{-1}. This indicates that the *trans*-Zr_2N_2 structure is thermodynamically stable compared to its starting structures (N_2 and Zr_2). Furthermore, the *trans* complex is 296.2 kJmol^{-1} more stable than the *cis*-complex. The Bader charge analysis[33] shows that Zr is oxidized and N is reduced by equal quantities retaining the net charge of the molecule zero.

Spectroscopic and theoretical studies of dinuclear zirconium complexes show that Zr_2N_2 core can be planar or bent based on the metal center or steric effect or cis/trans configuration.[34] However, there is no report available in the literature on the gas phase structures of *cis* and *trans*-Zr_2N_2.

B. The formation of Zr_2C_{60}, *cis*-$Zr_2N_2C_{60}$ and *trans*-$Zr_2N_2C_{60}$ complexes

In this section we discuss the structures, Bader charges and reaction energies of *cis*-$Zr_2N_2C_{60}$ and *trans*-$Zr_2N_2C_{60}$ complexes formed between the Zr_2C_{60} and N_2. The structure of a Zr dimer chemisorbed onto C_{60} (Zr_2C_{60}) was first calculated. Reaction energy for the formation of Zr_2 C_{60} from a C_{60} and a Zr dimer is calculated to be −223 kJ mol^{-1}. In the optimised structure, the Zr-Zr distance is 2.80 Å, which is longer than the free Zr dimer bond length of 2.01 Å. This indicates that the dimer must have a substantial interaction with C_{60}, since the final structure has a Zr-Zr interatomic distance almost 39% larger than the isolated Zr-Zr bond length. The optimised structure of Zr_2C_{60} together with bond distances and charge density plot is shown in Figure 2.

In the relaxed configuration, the Zr atoms form shortest Zr-C bonds with carbon atoms of the (6,6) bond. The closest Zr–C_{60} bond distances are calculated to be 2.27 Å and 2.29 Å. This indicates that strong Zr-C bonds are formed. The C-C bond elongation is also observed in the C_{60} due to the strong interaction of Zr_2 with C_{60}. From the Bader charge analysis, it is observed that the Zr dimer has been oxidized. Each Zr atom transfers 1.34 |*e*| to C_{60}.

In the next step, we calculated the structure and reaction energy of *cis*-$Zr_2N_2C_{60}$ from Zr_2C_{60} and N_2. The optimised structure with bond distances and cross sectional charge density plot are shown in Figure 3. The lateral interaction of N_2 on Zr_2C_{60} elongated the Zr-Zr bond distance further by 0.12 Å compared to the Zr dimer distance in Zr_2C_{60}. Furthermore the structure of Zr_2N_2 is slightly distorted. This is reflected in the unequal charge distribution on N atoms. In the optimised structure the N-N bond distance is 1.237 Å. The degree of activation in N≡N is similar compared to the activation observed in *cis*-Zr_2N_2 complex unsupported by C_{60}. The reaction energy for the formation of *cis*-$Zr_2N_2C_{60}$ from N_2 and Zr_2C_{60} is calculated to be −257.6 kJmol^{-1}. The formation of *cis* complex supported by C_{60} is facilitated further by 115 kJmol^{-1} indicating the necessity of stabilizing the Zr dimer on C_{60}.

Finally, we calculated the structure and reaction energy of *trans*-$Zr_2N_2C_{60}$ from Zr_2C_{60} and N_2. The optimised structure showing bond distances and Bader charges and cross sectional charge density plot are shown in Figure 4. The calculation reveals that the reaction is highly exothermic energy of −468 kJ mol^{-1}. This energy value is lower (by 28 kJmol^{-1}) than the formation energy calculated for *free* Zr_2N_2. In the presence of C_{60} the reaction energy is slightly favored. This result indicates that Zr_2 on the surface of C_{60} or a carbon nanotube would be a good choice for dinitrogen activation.

In the optimised *trans*-$Zr_2N_2C_{60}$ structure, the Zr-N bond distance is ~1.96 Å, which is close to the value observed in the free *trans*-Zr_2N_2. The Zr_2N_2 unit is slightly bent and forms a butterfly type structure when it is coordinated to C_{60}. Zr-Zr and N-N separations were calculated to be 2.72 Å and 2.50 Å respectively and the N-N separation is slightly shorter than the N-N separation of 2.72 Å in the free Zr_2N_2. The Zr-Zr separation is reduced by only 0.07 Å when the Zr_2N_2 unit is formed on C_{60} surface. The Bader charge analysis indicates that there is a greater charge transfer from Zr atoms to C_{60} and N atoms. Zr atoms have lost over all charge of 5.23 |e|. Two N atoms gained 3.83 |e| and C_{60} has gained remaining 1.40 |e|.

C. Reactions with hydrogen

The next step was to carry out additional calculations to look at the products of the reaction with H_2 to find possible routes for NH_3 formation. The first H_2 was allowed to react with *trans*-$Zr_2N_2C_{60}$ to give $Zr_2N_2H_2C_{60}$. The resulting geometry is given in Figure 5. The reaction energy for this reaction is calculated to be exothermic (energy change of −125.44 kJ mol^{-1}) suggesting that the hydrogenated product is thermodynamically stable. The Zr-N and N-H bond lengths are ~2.05 Å and 1.03 Å, respectively. The Zr-Zr and N-N separations are found to be 2.52 Å and 2.97 Å respectively.

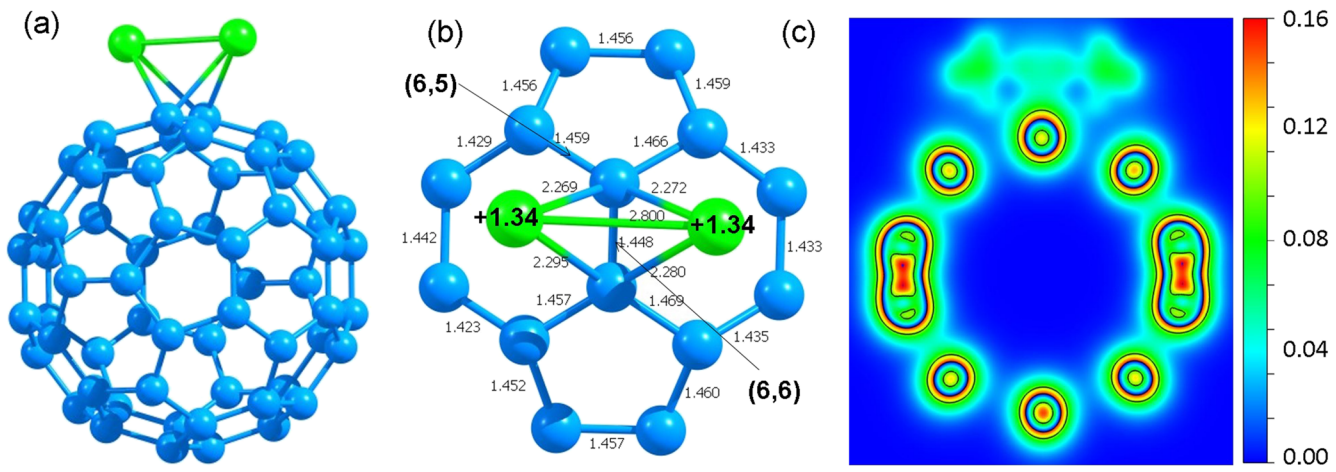

FIG. 2. (a) The optimised structure of Zr_2C_{60} (b) the expanded view structure showing bond distances and Bader charges on Zr atoms and (c) the cross sectional charge density plot showing the interaction of Zr dimer with C_{60}.

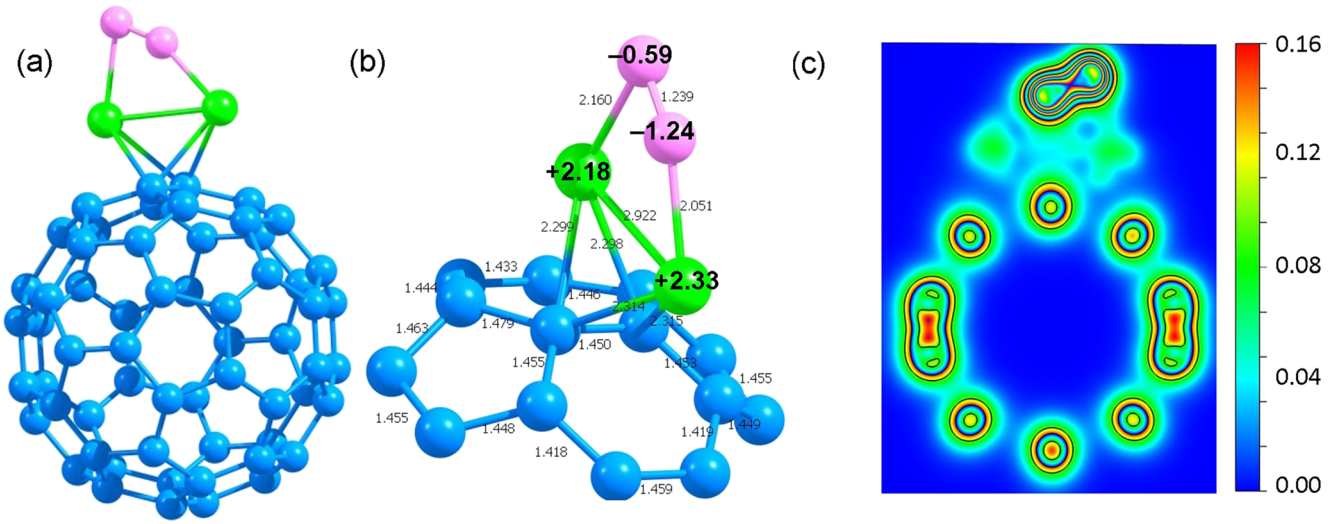

FIG. 3. (a) The optimised structure of *cis*-$Zr_2N_2C_{60}$, (b) the expanded view structure showing bond distances and Bader charges and (c) the cross sectional charge density plot showing the interaction of N_2 with Zr_2C_{60}.

Reaction of one mole of H_2 increases the N-N separation and decreases the Zr-Zr separation due to the greater charge on N atoms resulting from the donation of electron from H to N.

The second H_2 molecule was allowed to react with $Zr_2N_2H_2C_{60}$ to form $Zr_2N_2H_4C_{60}$. In the optimised structure, each N forms two strong bonds with hydrogen with the N-H distance of 1.03 Å and both NH_2 groups bridge the Zr_2 unit (refer to Figure 6). The Zr-Zr bond distance is slightly reduced to 2.49 Å. The Zr-N bond lengths are calculated to be 2.25 Å. Figure 6 shows the optimised structure of $Zr_2N_2H_4C_{60}$ together with bond distances, Bader charges on N and Ti atoms and charge density plot showing the interaction between $Zr_2N_2H_4$ and C_{60}.

The reaction energy for this route is exothermic and the value is −27.9 kJ mol^{-1} showing that the addition of the second H_2 molecule is thermodynamically favourable. Bader charge analysis indicates that the addition of H atoms increases the charge on N. This because of the electronegative N gain electron from H. This minimizes the positive charge on Zr atoms.

Next, we devise two possible routes for the formation of NH_3 by adding a third H_2 molecule with $Zr_2N_2H_4C_{60}$. In the first route two moles of NH_3 and one mole of catalyst Zr_2C_{60} are yielded as shown in the equation 2. This route is endothermic by as much as 409 kJ mol^{-1} and therefore it is unlikely.

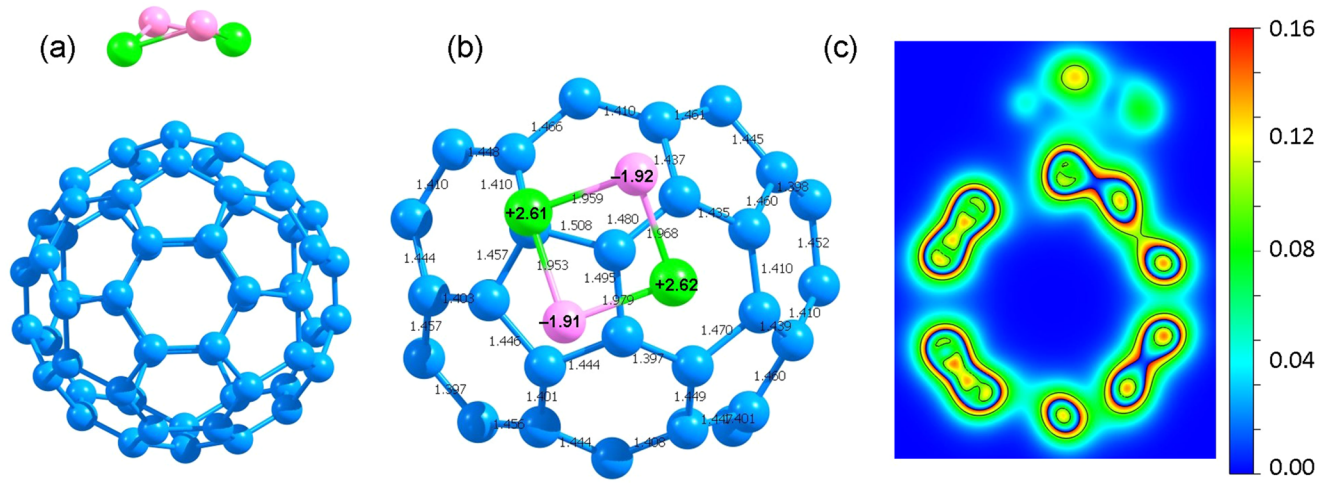

FIG. 4. (a) The optimised structure of *trans*-$Zr_2N_2C_{60}$ (b) the expanded view structure together with the bond distances and Bader charges and (c) the cross sectional charge density plot showing the interaction of N_2 with Zr_2C_{60}.

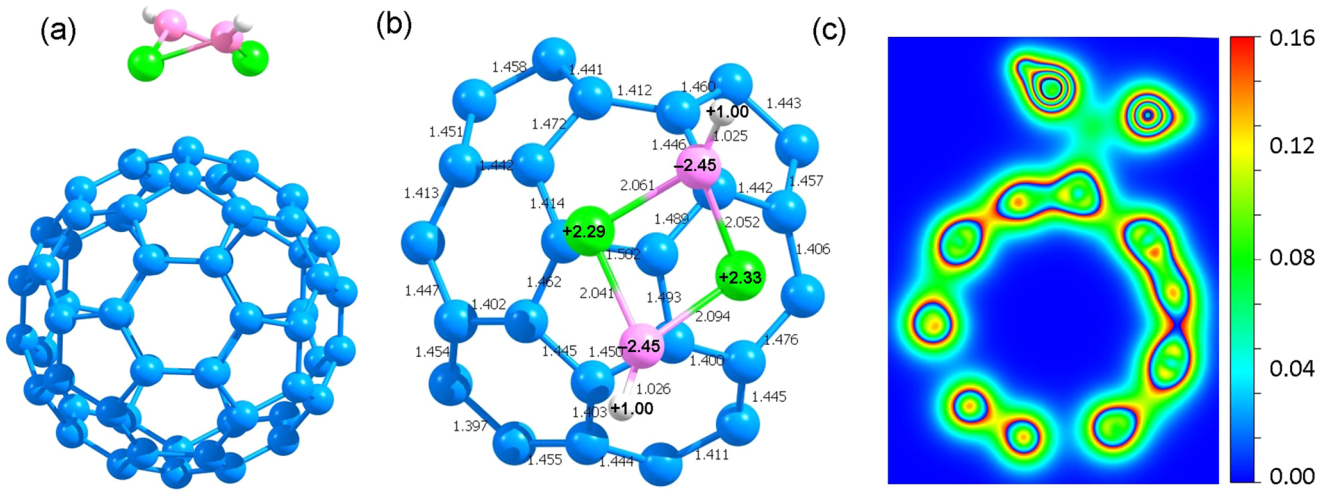

FIG. 5. (a) The optimised structure of $Zr_2N_2H_2C_{60}$, (b) the expanded view structure with bond distances and Bader charges and (c) the cross sectional charge density plot showing the interaction of $Zr_2N_2H_2$ with C_{60}.

$$Zr_2N_2H_4C_{60} + H_2 \rightarrow Zr_2C_{60} + 2NH_3 \quad (2)$$

In this reaction two moles of NH_3 and one mole of catalyst Zr_2C_{60} are yielded. This route is endothermic by as much as 409 kJ mol^{-1} and it is unlikely.

In the second route, there are two steps. In the first step, $Zr_2N_2H_4C_{60}$ reacts with one mole of H_2 to yield one mole of $Zr_2C_{60}(NH_2)H$ and one molecule of NH_3 according to the following equation.

$$Zr_2N_2H_4C_{60} + H_2 \rightarrow Zr_2(NH_2)HC_{60} + NH_3 \quad (3)$$

The structure of $Zr_2(NH_2)HC_{60}$ obtained as a product in the above reaction is shown in Figure 7. In the optimised structure, Zr-H, Zr-N, N-H and Zr-Zr bond distances were calculated to be 2.05 Å, 2.20/2.27 Å, 1.03 Å and 2.44 Å respectively.

In the second step, another mole of NH_3 and Zr_2C_{60} is yielded from $Zr_2(NH_2)HC_{60}$ according to the following equation:

$$Zr_2(NH_2)HC_{60} \rightarrow Zr_2C_{60} + NH_3 \quad (4)$$

The first step of the second route is endothermic by 123 kJ mol^{-1} and the reaction energy for the second step is calculated to be

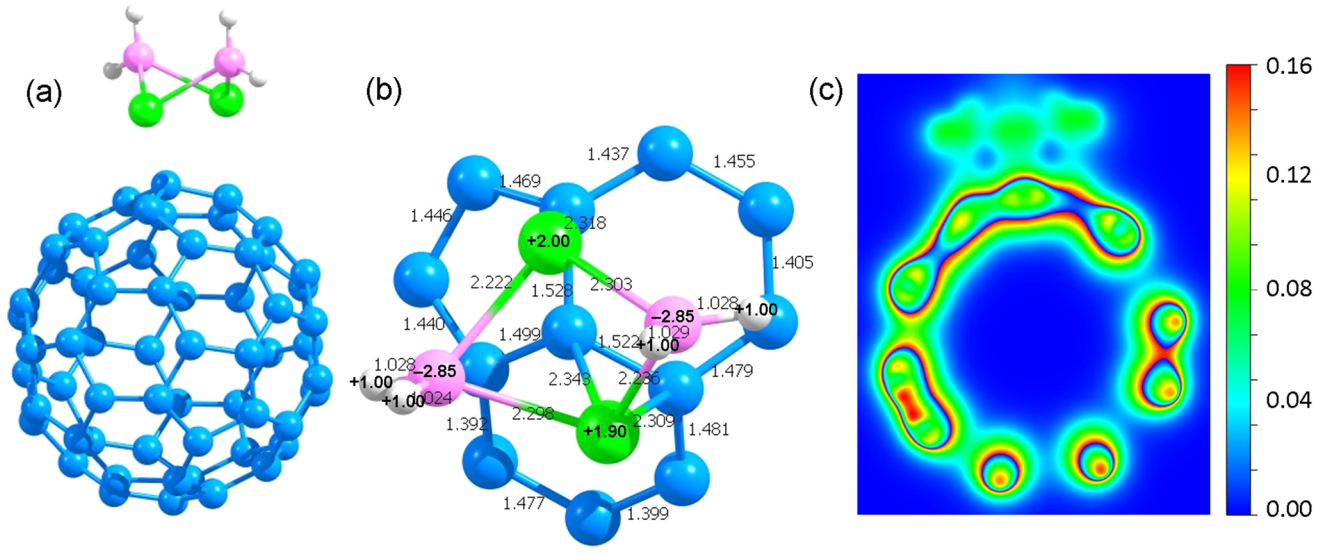

FIG. 6. (a) The optimised structure of $Zr_2N_2H_4C_{60}$ (b) the expanded view structure showing bond distances and Bader charges and (c) the cross sectional charge density plot showing the interaction of $Zr_2N_2H_4$ with C_{60}.

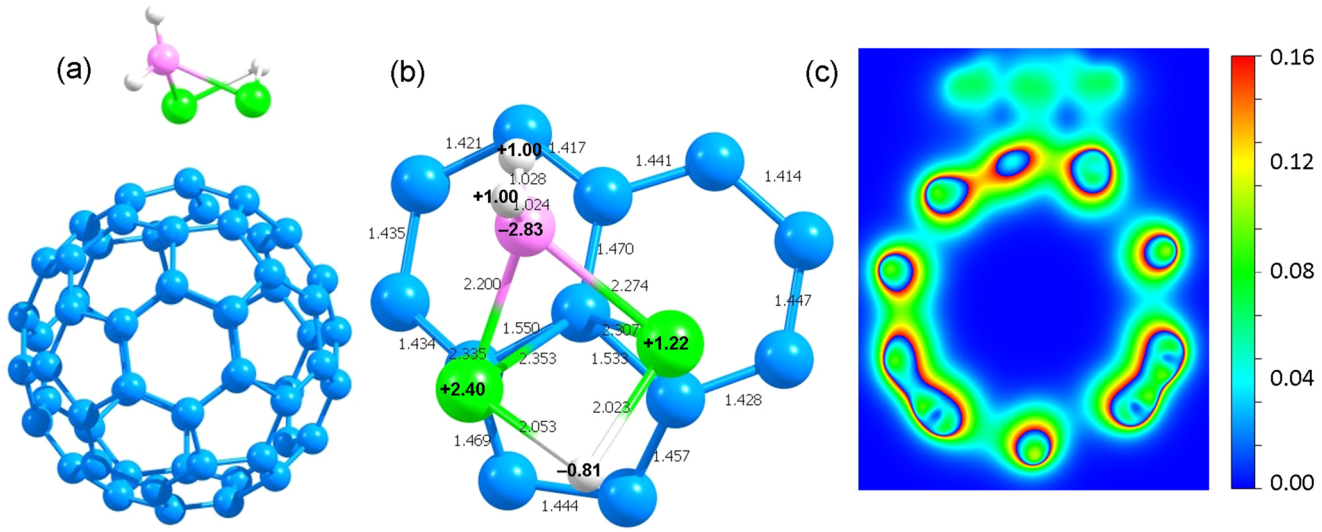

FIG. 7. (a) The optimised structure of $Zr_2(NH_2)HC_{60}$ (b) the expanded view structure together with bond distances and Bader charges and (c) the cross sectional charge density plot showing the interaction of $Zr_2(NH_2)H$ with C_{60}.

354 kJ mol^{-1}. Though this second step is unfavorable, if it were to be coupled with reaction with a further mole of N_2, the overall process would be exothermic. Figure 8 shows a catalytic cycle consisting of all reactions and relative energy diagram for the formation of intermediates during the reaction $N_2+3H_2 \rightarrow 2NH_3$ catalyzed by Zr_2C_{60}.

D. Hydrogenation of *trans*-Zr_2N_2 for the formation of NH_3 (uncatalysed)

Earlier we discussed the formation of *trans*-Zr_2N_2 from Zr_2 and N_2 in the absence of C_{60}. Here we discuss the reaction energies and products during the hydrogenation with *trans*-Zr_2N_2. The optimised structure of $Zr_2N_2H_2$ (refer to Figure 9a) is similar to

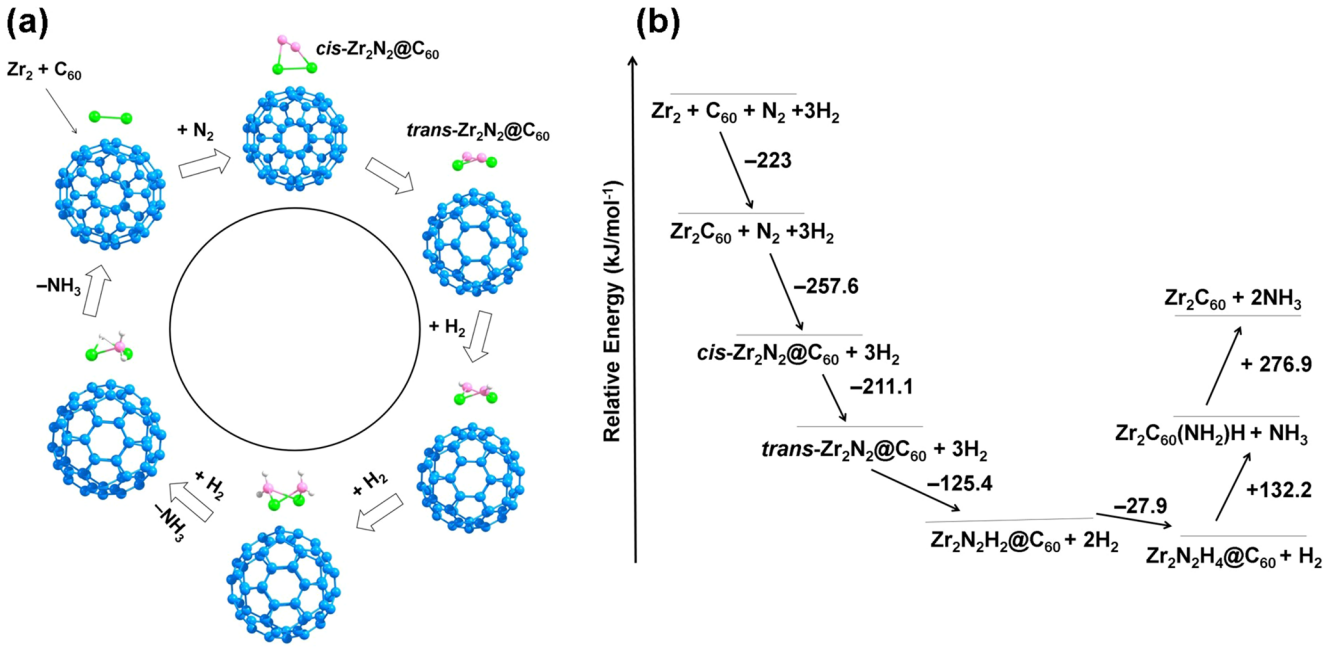

FIG. 8. (a) Catalytic cycle for the reduction of N_2 to NH_3 and (b) relative energies of intermediates formed during the reaction $N_2+3H_2 \rightarrow 2\ NH_3$ catalyzed by Zr_2C_{60}.

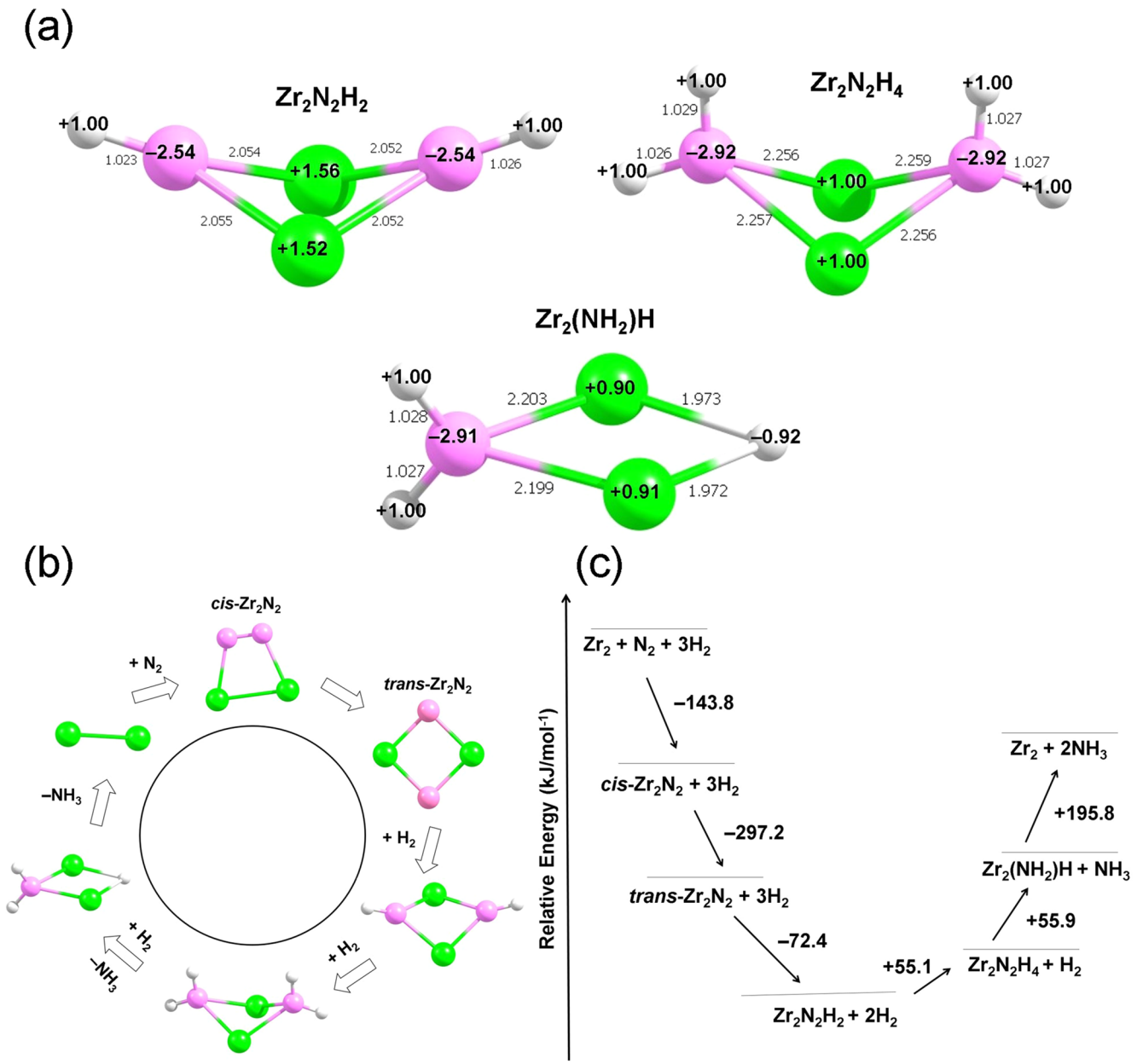

FIG. 9. (a) Optimised structures of hydrogenated products of *trans*-Zr_2N_2 together with Bader charges (b) catalytic cycle for the reduction of N_2 to NH_3 and (c) relative energies of intermediates formed during the reaction $N_2+3H_2 \rightarrow 2NH_3$.

that of the $Zr_2N_2H_2C_{60}$ and exhibits a butterfly shape. There is a slight reduction in the Zr-N bond distances. There is a significant reduction in the Bader charge on Zr atoms compared to those observed in $Zr_2N_2H_2C_{60}$ and this can be attributed to the greater charge transfer from the Zr dimer to C_{60}. The reaction energy for the formation of $Zr_2N_2H_2$ from N_2 and H_2 is exothermic (−72.4 kJmol^{-1}). The addition of the first H_2 molecule with Zr_2N_2 unit supported by C_{60} is highly exothermic (−125.4 kJmol^{-1}). This indicates that C_{60} facilitates the addition of the first H_2 molecule.

The addition of the second H_2 molecule introduces changes in the Zr-N bonds and Bader charges on Zr and N atoms. The optimised structure almost retains its butterfly shape. The Bader charge on each N increases due to the additional charge transfer from the second H. Furthermore, the charges on Zr atom also decreases due to the absence of C_{60}. The formation energy of free $Zr_2N_2H_4$ is

endothermic by 55.1 kJ mol^{-1} while with C_{60} the reaction energy is −27.9 kJ mol^{-1}. This clearly indicates the necessity of the stabilization of Zr dimer with C_{60}.

The energy of the first possible route for the formation of ammonia with the third H_2 ($Zr_2N_2H_4 + H_2 \rightarrow Zr_2 + 2NH_3$) was calculated. This route is endothermic by 252 kJ mol^{-1}. This reaction energy is lower by 157 kJmol^{-1} compared to the value calculated in the presence of C_{60}.

The first step of the second route [$Zr_2N_2H_4 + H_2 \rightarrow Zr_2(NH_2)H + NH_3$] was calculated. In the first step the reaction energy is endothermic by 55.9 kJ mol^{-1}. This value is lower by 76 kJ mol^{-1} than the value calculated in the presence of C_{60}. The optimised structure of $Zr_2(NH_2)H$ is planar (refer to Figure 9a) in contrast to the structure observed with $C_{60.}$ This is because of the asymmetric nature of $Zr_2(NH_2)H$ molecule and lower charge on Zr atoms compared to those observed in $Zr_2(NH_2)H$ C_{60}. In the second step, another moiety of NH_3 and Zr_2 is yielded from Zr_2NH_3. The reaction energy is endothermic by 195.8 kJ mol^{-1}. This value is +276.9 kJ mol^{-1} when this reaction is carried out in C_{60}.

IV. CONCLUSIONS

In the present study, the thermodynamic stability of Zr_2N_2 and $Zr_2N_2C_{60}$ structures and their hydrogenated configurations were calculated using density functional theory. The calculations show that the optimised *trans*-Ti_2N_2 configuration is planar but this configuration exhibits a butterfly shape when it is supported by C_{60}. Activation of dinitrogen is facilitated by the Zr dimer stabilized by C_{60}. The complete cleavage of the N≡N bond and highly exothermic formation energy in the reaction $Zr_2C_{60} + N_2 \rightarrow$ *trans*-$Zr_2N_2C_{60}$ show that C_{60} or a nanotube would be a candidate material to stabilize Zr dimer or Zr clusters to facilitate the dinitrogen activation. Consequent addition of two molecules of H_2 is exoergic in the process supported by C_{60} while only one molecule of H_2 can react exothermically with *trans*-Zr_2N_2 suggesting the necessity of stabilization with C_{60}.

ACKNOWLEDGMENTS

Computational facilities and support were provided by High Performance Computing Centre at Imperial College London.

The authors declare that there is no competing financial interest.

REFERENCES

[1] H.-J. Himmel and M. Reiher, Angewandte Chemie International Edition **45**, 6264 (2006).
[2] F. Haber and R. Le Rossignol, Zeitschrift für Elektrochemie und Angewandte Physikalische Chemie **14**, 513 (1908).
[3] B. K. Burgess, Chemical Reviews **90**, 1377 (1990).
[4] B. K. Burgess and D. J. Lowe, Chemical Reviews **96**, 2983 (1996).
[5] J. Kim and D. C. Rees, Biochemistry **33**, 389 (1994).
[6] M. D. Fryzuk, The Chemical Record **3**, 2 (2003).
[7] Y. Ohki and M. D. Fryzuk, Angewandte Chemie International Edition **46**, 3180 (2007).
[8] M. D. Fryzuk, Science **340**, 1530 (2013).
[9] S. Gambarotta, Journal of Organometallic Chemistry **500**, 117 (1995).
[10] H.-J. Himmel, O. Hübner, W. Klopper, and L. Manceron, Angewandte Chemie International Edition **45**, 2799 (2006).
[11] M. Zhou, X. Jin, Y. Gong, and J. Li, Angewandte Chemie International Edition **46**, 2911 (2007).
[12] H.-J. Himmel, O. Hübner, F. A. Bischoff, W. Klopper, and L. Manceron, Physical Chemistry Chemical Physics **8**, 2000 (2006).
[13] H.-J. Himmel and A. Bihlmeier, Chemistry–A European Journal **10**, 627 (2004).
[14] O. Hübner, H.-J. Himmel, L. Manceron, and W. Klopper, The Journal of Chemical Physics **121**, 7195 (2004).
[15] M. S. Dresselhaus, G. Dresselhaus, and P. C. Eklund, in *Science of Fullerenes and Carbon Nanotubes*, edited by M. S. Dresselhaus, G. Dresselhaus, and P. C. Eklund (Academic Press, San Diego, 1996), p. 60.
[16] H. W. Kroto, A. W. Allaf, and S. P. Balm, Chemical Reviews **91**, 1213 (1991).
[17] K. Lee, H. Song, and J. T. Park, Accounts of Chemical Research **36**, 78 (2003).
[18] S. Nagao, T. Kurikawa, K. Miyajima, A. Nakajima, and K. Kaya, The Journal of Physical Chemistry A **102**, 4495 (1998).
[19] O. Loboda, V. R. Jensen, and K. J. B∅rve, Fullerenes, Nanotubes and Carbon Nanostructures **14**, 365 (2006).
[20] N. Goldberg and R. Hoffmann, Journal of the American Chemical Society **118**, 3315 (1996).
[21] P. Karamanis and C. Pouchan, The Journal of Physical Chemistry C **116**, 11808 (2012).
[22] Q. Sun, Q. Wang, P. Jena, and Y. Kawazoe, Journal of the American Chemical Society **127**, 14582 (2005).
[23] N. Kuganathan, J. C. Green, and H.-J. Himmel, New Journal of Chemistry **30**, 1253 (2006).
[24] G. P. Kushto, P. F. Souter, G. V. Chertihin, and L. Andrews, The Journal of Chemical Physics **110**, 9020 (1999).
[25] G. Kresse and J. Furthmüller, Physical Review B **54**, 11169 (1996).
[26] G. Kresse and D. Joubert, Physical Review B **59**, 1758 (1999).
[27] J. P. Perdew, K. Burke, and M. Ernzerhof, Physical Review Letters **77**, 3865 (1996).
[28] W. H. Press, S. A. Teukolsky, W. T. Vetterling, and B. P. Flannery, *Numerical recipes in C* (2nd ed.): The art of scientific computing (Cambridge University Press, 1992).
[29] S. Grimme, J. Antony, S. Ehrlich, and H. Krieg, The Journal of Chemical Physics **132**, 154104 (2010).
[30] N. Kuganathan, A. K. Arya, M. J. D. Rushton, and R. W. Grimes, Carbon **132**, 477 (2018).
[31] M. Grunze, M. Golze, W. Hirschwald, H. J. Freund, H. Pulm, U. Seip, M. C. Tsai, G. Ertl, and J. Küppers, Physical Review Letters **53**, 850 (1984).
[32] J. M. H. Olmsted, G. M. Williams, and D. G. Friedman, *Chemistry: The molecular science* (Wm. C. Brown Publishers, Estados Unidos, 1997), p. 31.
[33] W. Tang, E. Sanville, and G. Henkelman, Journal of Physics: Condensed Matter **21**, 084204 (2009).
[34] F. Studt, L. Morello, N. Lehnert, M. D. Fryzuk, and F. Tuczek, Chemistry–A European Journal **9**, 520 (2003).